NANO LETTERS

pubs.acs.org/NanoLett Letter

Simultaneous Real-Time Three-Dimensional Localization and FRET Measurement of Two Distinct Particles

Xingxiang Chen,[○] Teng Liu,[○] Xianan Qin,[○] Quang Quan Nguyen, Sang Kwon Lee, Chanwoo Lee, Yaguang Ren, Jun Chu, Guang Zhu, Tae-Young Yoon, Chan Young Park, and Hyokeun Park*

Cite This: *Nano Lett.* 2021, 21, 7479−7485 Read Online

ACCESS | Metrics & More | Article Recommendations | Supporting Information

ABSTRACT: Many biological processes employ mechanisms involving the locations and interactions of multiple components. Given that most biological processes occur in three dimensions, the simultaneous measurement of three-dimensional locations and interactions is necessary. However, the simultaneous three-dimensional precise localization and measurement of interactions in real time remains challenging. Here, we report a new microscopy technique to localize two spectrally distinct particles in three dimensions with an accuracy (2.35σ) of tens of nanometers with an exposure time of 100 ms and to measure their real-time interactions using fluorescence resonance energy transfer (FRET) simultaneously. Using this microscope, we tracked two distinct vesicles containing t-SNAREs or v-SNARE in three dimensions and observed FRET simultaneously during single-vesicle fusion in real time, revealing the nanoscale motion and interactions of single vesicles in vesicle fusion. Thus, this study demonstrates that our microscope can provide detailed information about real-time three-dimensional nanoscale locations, motion, and interactions in biological processes.

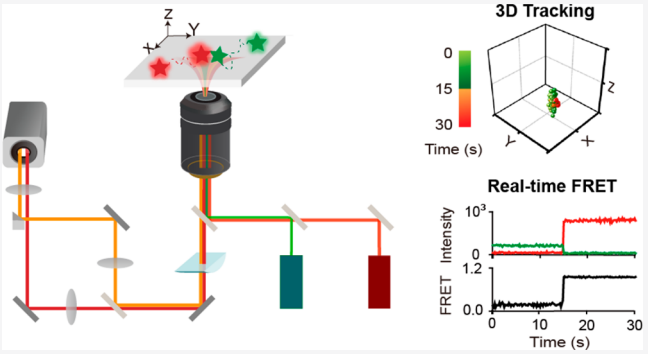

KEYWORDS: *single-particle tracking, FRET, nanometric precision, three-dimensional localization, vesicle fusion*

Recent advances in single-molecule fluorescence techniques enable us to observe the dynamics of individual proteins and organelles.[1−6] In particular, single-particle tracking allows us to monitor the motions of single proteins or organelles with high spatiotemporal resolution, and provides deeper understanding about underlying mechanisms in complex biological systems.[7−11] For example, two-dimensional single-particle tracking of membrane proteins on the plasma membrane has revealed the lateral motion of membrane proteins and their roles in the biological processes.[7,12−14] Given that most proteins and organelles move in three dimensions in biological systems, three-dimensional localization is required to accurately understand the locations and motion of these proteins and organelles. Recently, new methods to localize single particles in three dimensions have been developed and provided new information about biological processes with high spatiotemporal resolution.[4,11,15−37]

Fluorescence (or Förster) resonance energy transfer (FRET) has become a very powerful research tool in biology.[38] FRET is a process by which an excited donor fluorophore transfers its energy to an acceptor fluorophore through a dipole−dipole interaction.[38,39] FRET has been widely used for studying the nanometer-scale dynamics and protein−protein interactions in many biological systems.[40−44] In particular, single-molecule FRET enables us to observe the conformational changes and interactions of single proteins and nucleic acids,[39,41,45] whereas live-cell FRET allows us to study molecular interactions and the stoichiometry of donor and acceptor molecules in living cells.[46−48]

Since many biological processes are involved with the three-dimensional locations and interactions of multiple components, comprehensive understanding of biological processes requires the simultaneous measurement of their three-dimensional locations and interactions. However, the simultaneous measurement of three-dimensional locations and interactions of two particles remains challenging. Here, we have developed a new microscopy technique to simultaneously localize two spectrally distinct particles in three dimensions with nanometric precision and measure the interactions between them using FRET in real time.

In order to simultaneously localize two spectrally distinct particles in three dimensions and measure their interactions in real time, we built a dual-color three-dimensional localization

Received: April 1, 2021
Published: September 7, 2021

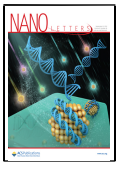

https://doi.org/10.1021/acs.nanolett.1c01328
Nano Lett. 2021, 21, 7479−7485

and FRET microscope (dual-color 3D localization-FRET microscope). Figure 1 shows the schematic diagram of our

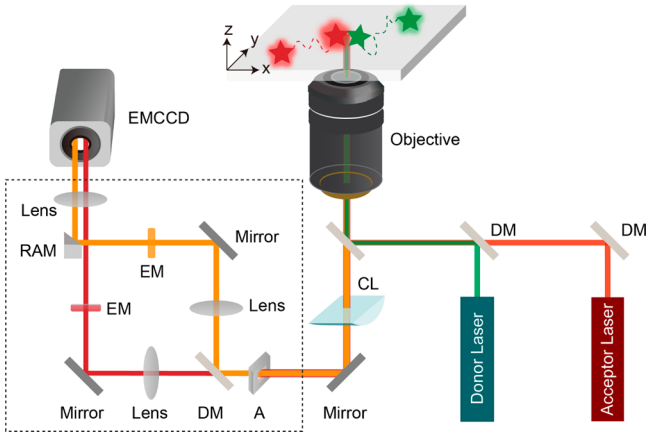

Figure 1. Schematicdiagram of a dual-color three-dimensional localization and FRET microscope (dual-color 3D localization-FRET microscope). A cylindrical lens (CL) is inserted into the emission path of the microscope to localize single particles in three dimensions. A custom-made dual-view imaging system (marked as a dashed rectangle) is used to split the whole emission signals into two spectrally distinct emission signals. The dual-view imaging system includes an aperture (A), a dichroic mirror (DM), a right-angle mirror (RAM), emission filters (EM), lenses and mirrors.

dual-color 3D localization-FRET microscope. To localize single particles in three dimensions, we used the astigmatism generated by a weak cylindrical lens (f = 10 m) which creates the varied ellipticity of a fluorophore at different z positions.[20,34,49] The ellipticity of the fluorophore depends on the position along the z-axis. The positions in the x−y plane and the widths of *point spread functions* (PSFs) of single fluorescent particles were obtained by fitting the fluorescence images to a two-dimensional Gaussian function defined as[20,50,51]

$$I(x, y) = A_0 + A_1 \exp\left[-\frac{1}{2}\left(\frac{x - x_0}{w_x}\right)^2 - \frac{1}{2}\left(\frac{y - y_0}{w_y}\right)^2\right] \quad (1)$$

where A_0 is the background, A_1 is the peak intensity of the PSF, x_0 and y_0 are the centroids in the x−y plane, and w_x and w_y are widths along the x-axis or y-axis, respectively. The x_0 and y_0 obtained from the two-dimensionalGaussian fitting can be used as the centroid position of fluorescent particles in the x−y plane. The calibration curve based on the widths of the PSFs or the ellipticity (w_x/w_y) at different z positions can be used to localize the z positions of fluorescent particles.[20,34,49,52] To localize three-dimensional positions of two spectrally distinct particles, we divided the whole emitted fluorescence signals into two spectrally distinct channels using a custom-made dual-view imaging system (Figure 1) and determined the three-dimensional positions of two spectrally distinct particles based on their PSF-fitting in each channel.

To test the accuracy of three-dimensional localization in two channels of our microscope, we used TetraSpeck microspheres containing many fluorophores. Figure 2a shows fluorescence images of TetraSpeck microspheres at different z positions in the donor channel (transmitting wavelength of 550−610 nm) and the acceptor channel (transmitting wavelength of 665−

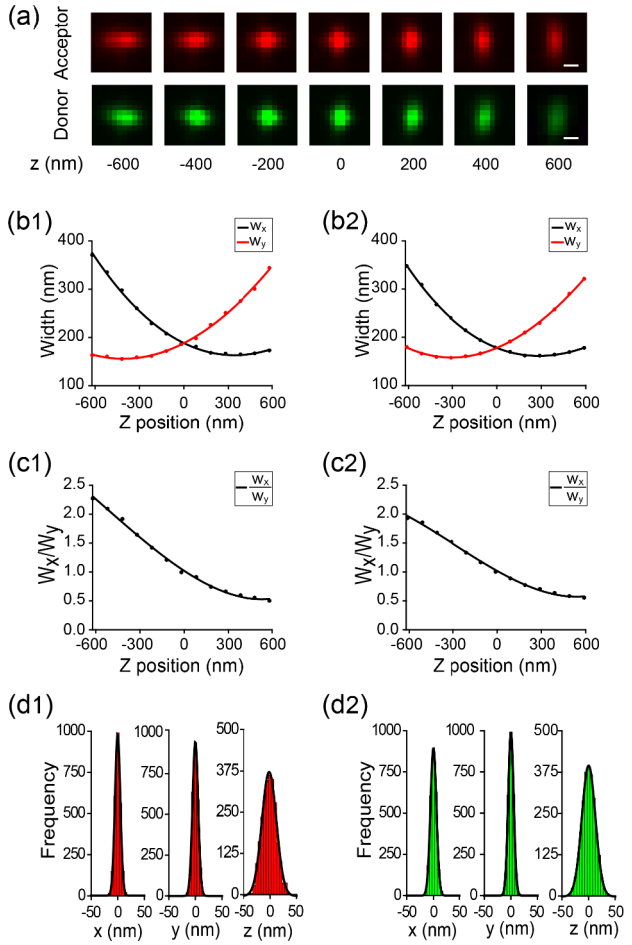

Figure 2. Three-dimensional localization of a single fluorescent microsphere. (a) Fluorescence images of a single TetraSpeck microsphere at different z positions in the donor and acceptor channels. The average fluorescence intensity of a single microsphere within a region of interest (ROI) in the donor channel was 979 whereas the average intensity of the same microsphere in the acceptor channel was 671. Scale bar: 500 nm. (b) Calibration curves based on the widths of the PSFs (w_x and w_y) at different positions along the z-axis in the acceptor (b1) and donor (b2) channels. (c) Calibration curves based on the ellipticity (w_x/w_y) at different z positions in the acceptor (c1) and donor (c2) channels. (d) Three-dimensional localization distribution of single microspheres in the acceptor and donor channels. Repeated localization of single PSFs yielded histograms. These histograms were fit to a Gaussian function, yielding standard deviations (σ) of 5.0 nm in x, 5.3 nm in y, and 13.7 nm in z in the acceptor channel (d1) and of 5.6 nm in x, 5.0 nm in y, and 12.7 nm in z in the donor channel (d2) with an exposure time of 100 ms.

715 nm) separated by a dichroic mirror (T647lpxr). Fluorescence images in both channels showed the strong dependence of the ellipticity of the fluorophores on the z position (Figure 2a) and were fitted into eq 1 to measure the widths of the PSF (w_x and w_y). The calibration curves based on the widths of the PSF (Figure 2b) or the ellipticity (w_x/w_y) (Figure 2c) at different z positions were used to localize the z positions of fluorophores. The localization accuracy was estimated by calculating the positional distributions with respect to the average position of each centroid.[16,20] The histograms of the localized positions were fitted to a Gaussian curve, which provided a standard deviation (σ) along the x-, y- and z-axes in these channels of this microscope. The localization accuracy of single TetraSpeck microspheres

https://doi.org/10.1021/acs.nanolett.1c01328
Nano Lett. 2021, 21, 7479−7485

estimated by full width at half-maximum (2.35σ) along the *x*-, *y*-, and *z*-axes was 11.8, 12.5, and 32.2 nm in the acceptor channel (Figure 2d1) and 13.2, 11.8, and 29.8 nm in the donor channel (Figure 2d2) with an exposure time of 100 ms, indicating that the dual-color 3D localization-FRET microscope can be used for localizing two spectrally distinct particles in three dimensions with nanometric precision. The localization accuracy in the *z* position is significantly worse than that in the *x* and *y* positions, which is consistent with previous reports.[16,20,33] The temporal resolution of the dual-color 3D localization-FRET microscope is limited by the readout rate of EMCCD camera and the number of collected photons. Since the lower number of collected photons during the exposure time of less than 100 ms resulted in a deterioration of the localization precision, we estimated 100 ms as the minimum exposure time for accurate three-dimensional tracking in our microscope. The range of axial localization in our dual-color 3D localization-FRET microscope was from −600 to 600 nm. The images of TetraSpeck microspheres were also used to generate a three-dimensional mapping file to register the locations of fluorophores in the acceptor channel onto the donor channel using 3D local weighted mean (LWM) transformation, similar to the previously reported two-dimensional mapping (see details in Supporting Information).[53,54]

To test whether our dual-color 3D localization-FRET microscope can be used for measuring real-time FRET, we performed real-time single-molecule FRET experiments. Figure 3a shows the schematic diagram of FRET measurement of single double-stranded DNA molecules labeled with ATTO 550 (donor) and ATTO 647N (acceptor) (see details in the Supporting Information). The biotin−NeutrAvidin interaction was used to immobilize biotinylated DNA molecules to the surface of a coverslip. Figure 3b shows fluorescence intensity time traces of a double-stranded DNA molecule labeled with ATTO 550 and ATTO 647N in the donor and acceptor channels excited by a 532 nm laser and separated by a dichroic mirror (T647lpx). The fluorescence intensity time traces of ATTO 550 and ATTO 647N show an *anti-correlated* behavior, which indicates the fluorescence resonance energy transfer between ATTO 550 and ATTO 647N molecules. We observed one-step photobleaching in the acceptor channel at 10 s, suggesting that the fluorescence in the acceptor channel was from a single ATTO 647N molecule. FRET efficiency is defined as the energy transfer fraction from a donor fluorophore to an acceptor fluorophore, and can be calculated in principle by the fraction of acceptor fluorescence intensity (I_{DA}) to the total fluorescence intensity of donor and acceptor ($I_{DD} + I_{DA}$) under the illumination of a donor excitation laser[41,55,56]

$$E = \frac{I_{DA}}{I_{DD} + I_{DA}} \tag{2}$$

The calculated real-time trace of FRET efficiency of single DNA molecules showed high-FRET efficiency (~0.9) between single ATTO 550 and ATTO 647N molecules before photobleaching of ATTO 647N (Figure 3c). This high FRET efficiency implies that ATTO 550 and ATTO 647N were in close proximity, which is in good agreement with our proximate labeling of ATTO 550 and ATTO 647N in the double-stranded DNA molecules. After photobleaching of ATTO 647N, the FRET efficiency decreased to nearly zero, indicating no FRET. Thus, the FRET measurement of single ATTO 550 and ATTO 647N labeled double-stranded DNA molecules demonstrates that our microscope can be used for measuring FRET efficiency between a donor fluorophore and an acceptor fluorophore in real time at the single-molecule level.

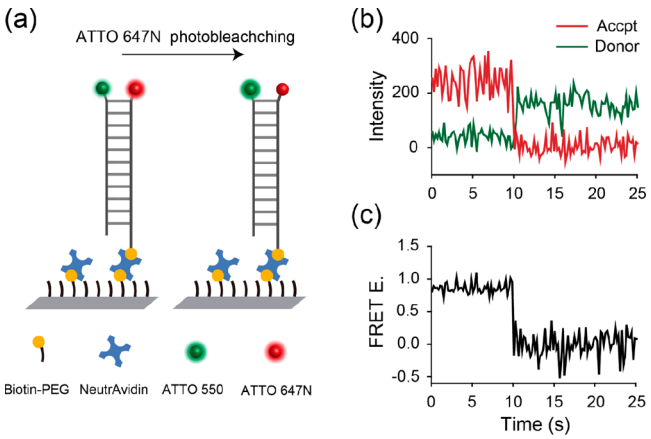

Figure 3. Single-molecule FRET of single double-stranded DNA molecules. (a) Schematics of immobilization. Biotinylated double-stranded DNA molecules containing ATTO 550 and ATTO 647N were immobilized to coverslips by the interaction between NeutrAvidin and biotinylated PEG (Biotin-PEG). (b) Fluorescence intensity time traces in the donor (ATTO 550) and acceptor (ATTO 647N) channels excited by a 532 nm laser. The fluorescence intensity trace in the ATTO 647N channel showed one-step photobleaching at 10 s, indicating that the fluorescence in the acceptor channel was from a single ATTO 647N molecule. (c) The trace of FRET efficiency shows that FRET efficiency decreased to almost zero after photobleaching of ATTO 647N.

Furthermore, we applied the dual-color 3D localization-FRET microscope to live-cell FRET using mClover3-mRuby3 FRET pair (a bright and photostable fluorescent proteins FRET pair)[57] in living HEK293T cells. We observed a significantly higher FRET efficiency of mClover3-2aa-mRuby3 compared with mClover3-80aa-mRuby3 (Supporting Figure S1), demonstrating the capability of this microscope to measure FRET in living cells.

To test whether the capability of the dual-color 3D localization-FRET microscope to simultaneously localize two spectrally distinct particles in three dimensions and to measure FRET between them can be used to study biological processes, we applied the dual-color 3D localization-FRET microscope to an *in vitro* single-vesicle fusion assay where two different types of reconstituted vesicles containing a FRET pair undergo membrane fusion using a set of *proteins called SNAREs* (soluble *N*-ethylmaleimide-sensitive factor attachment protein receptors).[58,59] We reconstituted one group of vesicles with target SNAREs (t-SNAREs) and the other group of vesicles with vesicle SNARE (v-SNARE). Due to the strong overlap between the emission spectrum of DiI (a yellow membrane-intercalating dye; donor) and the absorption spectrum of DiD (a red membrane-intercalating dye; acceptor) with Förster radius (R_0) = 5.2 nm,[60] a DiI-DiD FRET pair was used for measuring intervesicular FRET. Figure 4a shows the schematic diagram of the *in vitro* single-vesicle fusion assay (see detailed methods in the Supporting Information). Vesicles containing DiI and t-SNAREs (t-vesicles) were tethered to the surface of a coverslip through the interaction between the biotinylated lipid

https://doi.org/10.1021/acs.nanolett.1c01328
Nano Lett. 2021, 21, 7479−7485

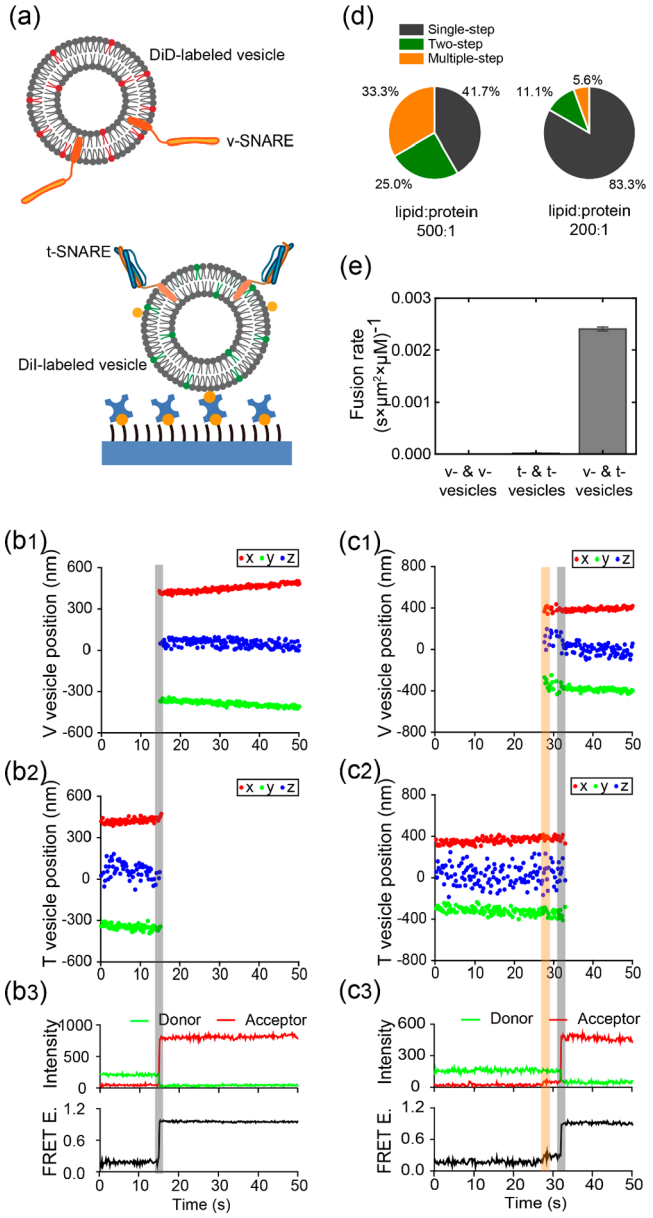

Figure 4. Simultaneous three-dimensional localization and FRET measurement of DiI-labeled and DiD-labeled vesicles in real time. (a) Schematic diagram of single DiI-labeled and DiD-labeled vesicles fusion assay. DiI-labeled vesicles containing t-SNAREs (t-vesicles) were immobilized to PEGylated coverslip using the NeutrAvidin–biotin interaction. DiD-labeled vesicles containing v-SNARE (v-vesicles) were added to a sample chamber to induce vesicle fusion. (b) Real-time three-dimensional trajectories of a single reconstituted DiD-labeled vesicle (b1) and a DiI-labeled vesicle (b2), fluorescence intensity time traces and a FRET efficiency trace (b3) showing one-step fusion without any intermediate step in vesicle fusion. Vertical gray bar: fusion. (c) Real-time three-dimensional trajectories, fluorescence intensity traces and a FRET efficiency trace showing two-step fusion with one intermediate. The intermediate represents the docking step. Vertical orange bar: docking. Vertical gray bar: fusion. (d) Prevalence of single-step, two-step and multiple-step fusion at different ratios of protein to lipid (1:500 (n = 24 fusion events) and 1:200 (n = 36 fusion events). (e) Fusion rate of vesicles by mixing t- and v-vesicle pair (N = 5 movies) or v-vesicles alone (N = 5 movies) or t-vesicles alone (N = 5 movies).

on the liposome membrane and NeutrAvidin bound to biotinylated polyethylene glycol (PEG) on the surface of the coverslip. After adding vesicles containing DiD and v-SNARE (v-vesicles), we observed the fusion between t-vesicles and v-vesicles using the dual-color 3D localization-FRET microscope. We illuminated these two types of vesicles using alternating illumination of 532 and 640 nm lasers with a 100 ms camera exposure time to simultaneously localize them in donor and acceptor channels and measure intervesicular FRET. A dichroic mirror (T647lpxr) was used for splitting fluorescence signals from vesicles labeled with DiI or DiD. Separate images of single vesicles containing DiI or DiD under alternate illumination of 532 or 640 nm lasers were used to localize these distinct vesicles in three dimensions in real time by fitting PSFs to eq 1 and by using the calibration curve. FRET efficiency was calculated by the ratio of acceptor intensity (I_{DA}) to the total intensity of donor and acceptor (I_{DD}+I_{DA}). Figure 4b–c display the three-dimensional trajectories, fluorescence intensity time traces, and FRET efficiency traces of vesicles undergoing different fusion pathways. Real-time three-dimensional trajectories and a FRET efficiency trace in Figure 4b show one-step fusion at 15.1 s, indicating that the v-vesicle (an acceptor vesicle) moved to the immobilized t-vesicle (a donor vesicle) and underwent rapid fusion without any intermediate step. Three-dimensional trajectories and a FRET efficiency trace in Figure 4c show two-step fusion, revealing one intermediate step before fusion. That is, the sudden increase of the acceptor fluorescence followed by a plateau in fluorescence intensity indicates that the v-vesicle moved suddenly toward the t-vesicle and underwent a docking step. Three-dimensional trajectories of the v-vesicle and the t-vesicle show that the centroids of two vesicles were located 42 nm away during the docking step. Then, these vesicles underwent full fusion at 32.1 s with the rapid increase of FRET efficiency. These traces reveal the detailed motion of single vesicles in the process of fusion. The combined three-dimensional trajectories of the v-vesicle and t-vesicle are shown in Figure S2. The motion of the v-vesicle was followed by the *anti-correlation* in fluorescence intensity between the v-vesicle and t-vesicle, implying that the motion of the v-vesicle toward the t-vesicle was closely trailed by the interactions between these pairs of the v-vesicle and t-vesicle. We also observed multiple-step fusion events (Figure S3), including three-step and four-step fusion, in the process of vesicle fusion. The prevalence of the one-step fusion event drastically increased at a higher ratio of protein to lipid (Figure 4d), which indicates that the high concentration of SNAREs in vesicles induces more full fusion without any intermediate step. Finally, control experiments further confirmed that vesicle-fusion was induced by mixing of v-vesicles and t-vesicles, not by mixing of the same types of vesicles (Figure 4e). Thus, the simultaneous three-dimensional tracking and FRET measurement of two distinct vesicles using the dual-color 3D localization-FRET microscope demonstrates its capability to provide detailed information about the dynamics of vesicle fusion from transport to full fusion, which has not been accessible with existing methods.

In this work, we introduce a new microscopy technique (dual-color 3D localization-FRET microscope), which enables us to simultaneously localize two spectrally distinct particles in three dimensions with nanometric precision and to measure FRET between them in biological processes in real time. Using this microscope, we observed the real-time three-dimensional nanoscale motion of single reconstituted vesicles in the process of vesicle fusion, which demonstrates the capability of this microscope to provide new dynamic information on three-

https://doi.org/10.1021/acs.nanolett.1c01328
Nano Lett. 2021, 21, 7479–7485

dimensional nanometric locations, motion, and their interactions of two particles in biological processes. Thus, this microscopy technique will be useful for investigating detailed mechanisms of biological processes because many biological processes are involved in simultaneous nanoscale motion and interactions in three dimensions. Furthermore, it can potentially be used for estimating a wide range of the distances between two particles in biological processes starting from a few nanometers to hundreds of nanometers. Owing to these capabilities, this dual-color 3D localization-FRET microscope will allow us to address important questions related to dynamic biological processes including how stromal interaction molecule 1 (STIM1 - a Ca^{2+} sensor in the endoplasmic reticulum (ER) membrane) and Orai1 (a Ca^{2+} release-activated Ca^{2+} channel subunit in the plasma membrane) move, bind each other, and activate store-operated Ca^{2+} channels at the ER-plasma membrane junction following depletion of Ca^{2+} store in the ER[14] and how G protein-coupled receptors (GPCRs) move and interact during the G-protein signaling in living cells.[61] Hence, the dual-color 3D localization-FRET microscopy will enable new discoveries about the dynamics and underlying mechanisms of biological processes.

■ ASSOCIATED CONTENT

Supporting Information

The Supporting Information is available free of charge at https://pubs.acs.org/doi/10.1021/acs.nanolett.1c01328.

Supporting figures and detailed experimental methods, including generation of plasmids, cell culture and transfection, fluorescence imaging, data analysis, three-dimensional registration, and single-vesicle fusion assay (PDF)

■ AUTHOR INFORMATION

Corresponding Author

Hyokeun Park − *Division of Life Science, Department of Physics, and State Key Laboratory of Molecular Neuroscience, The Hong Kong University of Science and Technology, Kowloon, Hong Kong;* orcid.org/0000-0002-2655-4795; Phone: (852) 2358-7322; Email: hkpark@ust.hk; Fax: (852) 2358-1552

Authors

Xingxiang Chen − *Division of Life Science, The Hong Kong University of Science and Technology, Kowloon, Hong Kong*

Teng Liu − *Department of Physics, The Hong Kong University of Science and Technology, Kowloon, Hong Kong*

Xianan Qin − *Department of Physics, The Hong Kong University of Science and Technology, Kowloon, Hong Kong;* Present Address: National Engineering Lab for Textile Fiber Materials & Processing Technology, College of Textile Science and Engineering, Zhejiang Sci-Tech University, Hangzhou 310018, China

Quang Quan Nguyen − *Department of Physics, The Hong Kong University of Science and Technology, Kowloon, Hong Kong*

Sang Kwon Lee − *Department of Biological Sciences, School of Life Sciences, UNIST, 44919 Ulsan, Republic of Korea*

Chanwoo Lee − *School of Biological Sciences and Institute of Molecular Biology and Genetics, Seoul National University, Seoul 08826, South Korea*

Yaguang Ren − *Department of Chemical and Biological Engineering, The Hong Kong University of Science and Technology, Kowloon, Hong Kong*

Jun Chu − *Research Lab for Biomedical Optics and Molecular Imaging, Shenzhen Institutes of Advanced Technology, Chinese Academy of Sciences, Shenzhen 518055, China*

Guang Zhu − *Division of Life Science and Department of Chemical and Biological Engineering, The Hong Kong University of Science and Technology, Kowloon, Hong Kong;* orcid.org/0000-0003-3802-3446

Tae-Young Yoon − *School of Biological Sciences and Institute of Molecular Biology and Genetics, Seoul National University, Seoul 08826, South Korea;* orcid.org/0000-0002-5184-7725

Chan Young Park − *Department of Biological Sciences, School of Life Sciences, UNIST, 44919 Ulsan, Republic of Korea*

Complete contact information is available at: https://pubs.acs.org/10.1021/acs.nanolett.1c01328

Author Contributions

X.C., T.L., X.Q., and H.P. designed the experiments. X.C., T.L., X.Q., Q.Q.N., S.K.L., C.L., and Y.R. performed the experiments. X.C., T.L., X.Q., and Q.Q.N. analyzed the data. X.C., T.L., X.Q., Q.Q.N., S.K.L., C.L., T.Y.Y., C.Y.P., and HP interpreted the data. S.K.L. and J.C. generated and provided the constructs. C.L. provided the proteins. X.C., T.L., X.Q., S.K.L., C.Y.P., and H.P. wrote the manuscript. G.Z., T.Y.Y., C.Y.P., and H.P. supervised students.

Author Contributions

○X.C., T.L., and X.Q. contributed equally to this work.

Notes

The authors declare no competing financial interest.

■ ACKNOWLEDGMENTS

We thank members of Park lab for helpful discussion and comments. This work was supported by grants from the Research Grants Council of Hong Kong (26101117, 16101518, N_HKUST613/17, and A-HKUST603/17 to H.P.), the Innovation and Technology Commission (ITCPD/17-9 to H.P.), National Natural Science Foundation of China (NSFC) (81927803 to J.C.), the National Research Foundation Grants (NRF-2016H1A2A1909031 to S.K.L., NRF-2019R1A2C2002235 and NRF-2018R1A5A1024340 to C.Y.P.), and the 2021 Joint Research Project of Institutes of Science and Technology (to C.Y.P.).

■ REFERENCES

(1) Park, H.; Toprak, E.; Selvin, P. R. Single-molecule fluorescence to study molecular motors. *Q. Rev. Biophys.* **2007**, *40* (1), 87−111.

(2) Joo, C.; Balci, H.; Ishitsuka, Y.; Buranachai, C.; Ha, T. Advances in single-molecule fluorescence methods for molecular biology. *Annu. Rev. Biochem.* **2008**, *77*, 51−76.

(3) Jung, S. R.; Fujimoto, B. S.; Chiu, D. T. Quantitative microscopy based on single-molecule fluorescence. *Curr. Opin. Chem. Biol.* **2017**, *39*, 64−73.

(4) von Diezmann, A.; Shechtman, Y.; Moerner, W. E. Three-Dimensional Localization of Single Molecules for Super-Resolution Imaging and Single-Particle Tracking. *Chem. Rev.* **2017**, *117* (11), 7244−7275.

(5) Miller, H.; Zhou, Z.; Shepherd, J.; Wollman, A. J. M.; Leake, M. C. Single-molecule techniques in biophysics: a review of the progress in methods and applications. Reports on progress in physics. *Rep. Prog. Phys.* **2018**, *81* (2), 024601.

(6) Izeddin, I.; El Beheiry, M.; Andilla, J.; Ciepielewski, D.; Darzacq, X.; Dahan, M. PSF shaping using adaptive optics for three-dimensional single-molecule super-resolution imaging and tracking. *Opt. Express* **2012**, *20* (5), 4957−67.
(7) Saxton, M. J.; Jacobson, K. SINGLE-PARTICLE TRACKING: Applications to Membrane Dynamics. *Annu. Rev. Biophys. Biomol. Struct.* **1997**, *26*, 373−399.
(8) Kusumi, A.; Tsunoyama, T. A.; Hirosawa, K. M.; Kasai, R. S.; Fujiwara, T. K. Tracking single molecules at work in living cells. *Nat. Chem. Biol.* **2014**, *10* (7), 524−32.
(9) Manzo, C.; Garcia-Parajo, M. F. A review of progress in single particle tracking: from methods to biophysical insights. Reports on progress in physics. *Rep. Prog. Phys.* **2015**, *78* (12), 124601.
(10) Shen, H.; Tauzin, L. J.; Baiyasi, R.; Wang, W.; Moringo, N.; Shuang, B.; Landes, C. F. Single Particle Tracking: From Theory to Biophysical Applications. *Chem. Rev.* **2017**, *117* (11), 7331−7376.
(11) Yu, C.; Zhang, M.; Qin, X.; Yang, X.; Park, H. Real-time imaging of single synaptic vesicles in live neurons. *Front. Biol.* **2016**, *11* (2), 109−118.
(12) Kusumi, A.; Nakada, C.; Ritchie, K.; Murase, K.; Suzuki, K.; Murakoshi, H.; Kasai, R. S.; Kondo, J.; Fujiwara, T. Paradigm shift of the plasma membrane concept from the two-dimensional continuum fluid to the partitioned fluid: high-speed single-molecule tracking of membrane molecules. *Annu. Rev. Biophys. Biomol. Struct.* **2005**, *34*, 351−78.
(13) Alcor, D.; Gouzer, G.; Triller, A. Single-particle tracking methods for the study of membrane receptors dynamics. *European journal of neuroscience* **2009**, *30* (6), 987−97.
(14) Qin, X.; Liu, L.; Lee, S. K.; Alsina, A.; Liu, T.; Wu, C.; Park, H.; Yu, C.; Kim, H.; Chu, J.; Triller, A.; Tang, B. Z.; Hyeon, C.; Park, C. Y.; Park, H. Increased Confinement and Polydispersity of STIM1 and Orai1 after Ca(2+) Store Depletion. *Biophys. J.* **2020**, *118* (1), 70−84.
(15) Park, C.; Chen, X.; Tian, C. L.; Park, G. N.; Chenouard, N.; Lee, H.; Yeo, X. Y.; Jung, S.; Tsien, R. W.; Bi, G. Q.; Park, H. Unique dynamics and exocytosis properties of GABAergic synaptic vesicles revealed by three-dimensional single vesicle tracking. *Proc. Natl. Acad. Sci. U. S. A.* **2021**, *118* (9), No. e2022133118.
(16) Park, H.; Li, Y.; Tsien, R. W. Influence of synaptic vesicle position on release probability and exocytotic fusion mode. *Science (Washington, DC, U. S.)* **2012**, *335* (6074), 1362−6.
(17) Levi, V.; Ruan, Q.; Kis-Petikova, K.; Gratton, E. Scanning FCS, a novel method for three-dimensional particle tracking. *Biochem. Soc. Trans.* **2003**, *31* (5), 997−1000.
(18) Toprak, E.; Balci, H.; Blehm, B. H.; Selvin, P. R. Three-Dimensional Particle Tracking via Bifocal Imaging. *Nano Lett.* **2007**, *7* (7), 2043−2045.
(19) Watanabe, T. M.; Sato, T.; Gonda, K.; Higuchi, H. Three-dimensional nanometry of vesicle transport in living cells using dual-focus imaging optics. *Biochem. Biophys. Res. Commun.* **2007**, *359*, 1−7.
(20) Huang, B.; Wang, W.; Bates, M.; Zhuang, X. Three-Dimensional Super-Resolution Imaging by Stochastic Optical Reconstruction Microscopy. *Science (Washington, DC, U. S.)* **2008**, *319*, 810−813.
(21) Pavani, S. R. P.; Thompson, M. A.; Biteen, J. S.; Lord, S. J.; Liu, N.; Twieg, R. J.; Piestun, R.; Moerner, W. E. Three-dimensional, single-molecule fluorescence imaging beyond the diffraction limit by using a double-helix point spread function. *Proc. Natl. Acad. Sci. U. S. A.* **2009**, *106* (9), 2995−2999.
(22) Shtengel, G.; Galbraith, J. A.; Galbraith, C. G.; Lippincott-Schwartz, J.; Gillette, J. M.; Manley, S.; Sougrat, R.; Waterman, C. M.; Kanchanawong, P.; Davidson, M. W.; Fetter, R. D.; Hess, H. F. Interferometric fluorescent super-resolution microscopy resolves 3D cellular ultrastructure. *Proc. Natl. Acad. Sci. U. S. A.* **2009**, *106* (9), 3125−30.
(23) Wells, N. P.; Lessard, G. A.; Goodwin, P. M.; Phipps, M. E.; Cutler, P. J.; Lidke, D. S.; Wilson, B. S.; Werner, J. H. Time-resolved three-dimensional molecular tracking in live cells. *Nano Lett.* **2010**, *10* (11), 4732−7.
(24) Aquino, D.; Schönle, A.; Geisler, C.; Middendorff, C. V.; Wurm, C. A.; Okamura, Y.; Lang, T.; Hell, S. W.; Egner, A. Two-color nanoscopy of three-dimensional volumes by 4Pi detection of stochastically switched fluorophores. *Nat. Methods* **2011**, *8* (4), 353−9.
(25) Dupont, A.; Lamb, D. C. Nanoscale three-dimensional single particle tracking. *Nanoscale* **2011**, *3* (11), 4532−41.
(26) Han, J. J.; Kiss, C.; Bradbury, A. R.; Werner, J. H. Time-resolved, confocal single-molecule tracking of individual organic dyes and fluorescent proteins in three dimensions. *ACS Nano* **2012**, *6* (10), 8922−32.
(27) Perillo, E. P.; Liu, Y. L.; Huynh, K.; Liu, C.; Chou, C. K.; Hung, M. C.; Yeh, H. C.; Dunn, A. K. Deep and high-resolution three-dimensional tracking of single particles using nonlinear and multiplexed illumination. *Nat. Commun.* **2015**, *6*, 7874.
(28) Duocastella, M.; Theriault, C.; Arnold, C. B. Three-dimensional particle tracking via tunable color-encoded multiplexing. *Opt. Lett.* **2016**, *41* (5), 863−6.
(29) Wang, G.; Hauver, J.; Thomas, Z.; Darst, S. A.; Pertsinidis, A. Single-Molecule Real-Time 3D Imaging of the Transcription Cycle by Modulation Interferometry. *Cell* **2016**, *167* (7), 1839−1852e.21.
(30) Hou, S.; Lang, X.; Welsher, K. Robust real-time 3D single-particle tracking using a dynamically moving laser spot. *Opt. Lett.* **2017**, *42* (12), 2390−2393.
(31) Qin, X.; Tsien, R. W.; Park, H. Real-time three-dimensional tracking of single synaptic vesicles reveals that synaptic vesicles undergoing kiss-and-run fusion remain close to their original fusion site before reuse. *Biochem. Biophys. Res. Commun.* **2019**, *514* (3), 1004−1008.
(32) Liu, Y. L.; Perillo, E. P.; Ang, P.; Kim, M.; Nguyen, D. T.; Blocher, K.; Chen, Y. A.; Liu, C.; Hassan, A. M.; Vu, H. T.; Chen, Y. I.; Dunn, A. K.; Yeh, H. C. Three-Dimensional Two-Color Dual-Particle Tracking Microscope for Monitoring DNA Conformational Changes and Nanoparticle Landings on Live Cells. *ACS Nano* **2020**, *14* (7), 7927−7939.
(33) Keller, A. M.; DeVore, M. S.; Stich, D. G.; Vu, D. M.; Causgrove, T.; Werner, J. H. Multicolor Three-Dimensional Tracking for Single-Molecule Fluorescence Resonance Energy Transfer Measurements. *Anal. Chem.* **2018**, *90* (10), 6109−6115.
(34) Holtzer, L.; Meckel, T.; Schmidt, T. Nanometric three-dimensional tracking of individual quantum dots in cells. *Appl. Phys. Lett.* **2007**, *90*, 053902.
(35) Juette, M. F.; Bewersdorf, J. Three-dimensional tracking of single fluorescent particles with submillisecond temporal resolution. *Nano Lett.* **2010**, *10* (11), 4657−63.
(36) Juette, M. F.; Gould, T. J.; Lessard, M. D.; Mlodzianoski, M. J.; Nagpure, B. S.; Bennett, B. T.; Hess, S. T.; Bewersdorf, J. Three-dimensional sub-100 nm resolution fluorescence microscopy of thick samples. *Nat. Methods* **2008**, *5* (6), 527−529.
(37) Hou, S.; Exell, J.; Welsher, K. Real-time 3D single molecule tracking. *Nat. Commun.* **2020**, *11* (1), 3607.
(38) Okamoto, K.; Sako, Y. Recent advances in FRET for the study of protein interactions and dynamics. *Curr. Opin. Struct. Biol.* **2017**, *46*, 16−23.
(39) Roy, R.; Hohng, S.; Ha, T. A practical guide to single-molecule FRET. *Nat. Methods* **2008**, *5* (6), 507−16.
(40) Lee, S. K.; Lee, M. H.; Jeong, S. J.; Qin, X.; Lee, A. R.; Park, H.; Park, C. Y. The inactivation domain of STIM1 acts through intramolecular binding to the coiled-coil domain in the resting state. *Journal of Cell Science* **2020**, *133* (1), No. jcs237354.
(41) Sasmal, D. K.; Pulido, L. E.; Kasal, S.; Huang, J. Single-molecule fluorescence resonance energy transfer in molecular biology. *Nanoscale* **2016**, *8* (48), 19928−19944.
(42) Aoki, K.; Kamioka, Y.; Matsuda, M. Fluorescence resonance energy transfer imaging of cell signaling from in vitro to in vivo: basis of biosensor construction, live imaging, and image processing. *Development, growth & differentiation* **2013**, *55* (4), 515−22.
(43) Ha, T. Single-molecule fluorescence resonance energy transfer. *Methods (Amsterdam, Neth.)* **2001**, *25* (1), 78−86.

https://doi.org/10.1021/acs.nanolett.1c01328
Nano Lett. 2021, 21, 7479−7485

(44) Tian, F.; Lin, T. C.; Wang, L.; Chen, S.; Chen, X.; Yiu, P. M.; Tsui, O. K. C.; Chu, J.; Kiang, C. H.; Park, H. Mechanical Responses of Breast Cancer Cells to Substrates of Varying Stiffness Revealed by Single-Cell Measurements. *J. Phys. Chem. Lett.* **2020**, *11* (18), 7643−7649.
(45) Lerner, E.; Cordes, T.; Ingargiola, A.; Alhadid, Y.; Chung, S.; Michalet, X.; Weiss, S. Toward dynamic structural biology: Two decades of single-molecule Forster resonance energy transfer. *Science (Washington, DC, U. S.)* **2018**, *359* (6373), eaan1133.
(46) Hoppe, A. D.; Shorte, S. L.; Swanson, J. A.; Heintzmann, R. Three-dimensional FRET reconstruction microscopy for analysis of dynamic molecular interactions in live cells. *Biophys. J.* **2008**, *95* (1), 400−18.
(47) Vogel, S. S.; Thaler, C.; Koushik, S. V. Fanciful FRET. *Sci. Signaling* **2006**, *2006* (331), No. re2.
(48) Sekar, R. B.; Periasamy, A. Fluorescence resonance energy transfer (FRET) microscopy imaging of live cell protein localizations. *J. Cell Biol.* **2003**, *160* (5), 629−33.
(49) Spille, J. H.; Kaminski, T.; Königshoven, H. P.; Kubitscheck, U. Dynamic three-dimensional tracking of single fluorescent nanoparticles deep inside living tissue. *Opt. Express* **2012**, *20* (18), 19697−707.
(50) Park, H.; Hanson, G. T.; Duff, S. R.; Selvin, P. R. Nanometre localization of single ReAsH molecules. *J. Microsc.* **2004**, *216* (3), 199−205.
(51) Selvin, P. R.; Lougheed, T.; Hoffman, M. T.; Park, H.; Balci, H.; Blehm, B. H.; Toprak, E. In vitro and in vivo FIONA and other acronyms for watching molecular motors walk. In *Single-Molecule Techniques: A Laboratory Manual*; Selvin, P. R., Ha, T., Eds.; Cold Spring Harbor Press: Cold Spring Harbor, NY, 2008; pp 37−71.
(52) Tafteh, R.; Abraham, L.; Seo, D.; Lu, H. Y.; Gold, M. R.; Chou, K. C. Real-time 3D stabilization of a super-resolution microscope using an electrically tunable lens. *Opt. Express* **2016**, *24* (20), 22959−22970.
(53) Qin, X.; Yoo, H.; Man Cheng, H. C.; Nguyen, Q. Q.; Li, J.; Liu, X.; Prunetti, L.; Chen, X.; Liu, T.; Sweeney, H. L.; Park, H. Simultaneous tracking of two motor domains reveals near simultaneous steps and stutter steps of myosin 10 on actin filament bundles. *Biochem. Biophys. Res. Commun.* **2020**, *525*, 94−99.
(54) Churchman, L. S.; Spudich, J. A. Colocalization of fluorescent probes: accurate and precise registration with nanometer resolution. *Cold Spring Harbor protocols* **2012**, *2012* (2), 141−9.
(55) Andoy, N. M.; Sarkar, S. K.; Wang, Q.; Panda, D.; Benitez, J. J.; Kalininskiy, A.; Chen, P. Single-molecule study of metalloregulator CueR-DNA interactions using engineered Holliday junctions. *Biophys. J.* **2009**, *97* (3), 844−52.
(56) McCann, J. J.; Choi, U. B.; Zheng, L.; Weninger, K.; Bowen, M. E. Optimizing methods to recover absolute FRET efficiency from immobilized single molecules. *Biophys. J.* **2010**, *99* (3), 961−70.
(57) Bajar, B. T.; Wang, E. S.; Lam, A. J.; Kim, B. B.; Jacobs, C. L.; Howe, E. S.; Davidson, M. W.; Lin, M. Z.; Chu, J. Improving brightness and photostability of green and red fluorescent proteins for live cell imaging and FRET reporting. *Sci. Rep.* **2016**, *6*, 20889.
(58) Yoon, T. Y.; Okumus, B.; Zhang, F.; Shin, Y. K.; Ha, T. Multiple intermediates in SNARE-induced membrane fusion. *Proc. Natl. Acad. Sci. U. S. A.* **2006**, *103* (52), 19731−6.
(59) Brunger, A. T.; Weninger, K.; Bowen, M.; Chu, S. Single-molecule studies of the neuronal SNARE fusion machinery. *Annu. Rev. Biochem.* **2009**, *78*, 903−28.
(60) Gravier, J.; Sancey, L.; Hirsjärvi, S.; Rustique, E.; Passirani, C.; Benoît, J. P.; Coll, J. L.; Texier, I. FRET imaging approaches for in vitro and in vivo characterization of synthetic lipid nanoparticles. *Mol. Pharmaceutics* **2014**, *11* (9), 3133−44.
(61) Vilardaga, J. P.; Agnati, L. F.; Fuxe, K.; Ciruela, F. G-protein-coupled receptor heteromer dynamics. *J. Cell Sci.* **2010**, *123* (24), 4215−20.

https://doi.org/10.1021/acs.nanolett.1c01328
Nano Lett. 2021, 21, 7479−7485